Published in final edited form as:

Nat Med. 2023 June ; 29(6): 1364–1369. doi:10.1038/s41591-023-02387-4.

Immune reconstitution inflammatory syndrome drives emergence of HIV drug resistance from multiple anatomic compartments in a person living with HIV

Andrea Lisco[1,12], **Camille Lange**[2,11,12,✉], **Maura Manion**[1], **Safia Kuriakose**[3], **Robin Dewar**[4], **Robert J. Gorelick**[5], **Kristi Huik**[2], **Quan Yu**[6], **Dima A. Hammoud**[7], **Bryan R. Smith**[8], **Pawel Muranski**[6], **Catherine Rehm**[1], **Brad T. Sherman**[9], **Craig Sykes**[10], **Natalie Lindo**[2], **Peiying Ye**[1], **Katherine M. Bricker**[1], **Brandon F. Keele**[5], **Christine M. Fennessey**[5], **Frank Maldarelli**[2,12,✉], **Irini Sereti**[1,12,✉]

[1]Laboratory of Immunoregulation, National Institute of Allergy and Infectious Diseases, National Institutes of Health, Bethesda, MD, USA.

[2]Clinical Retrovirology Section, HIV Dynamics and Replication Program National Cancer Institute, National Institutes of Health, Frederick, MD, USA.

[3]Clinical Research Directorate, Frederick National Laboratory for Cancer Research, Bethesda, MD, USA.

[4]Virus Isolation and Serology Laboratory, Frederick National Laboratory for Cancer Research, Frederick, MD, USA.

[5]AIDS and Cancer Virus Program, Frederick National Laboratory for Cancer Research, Frederick, MD, USA.

[6]Hematology Branch, National Heart, Lung and Blood Institute, National Institutes of Health, Bethesda, MD, USA.

✉**Correspondence and requests for materials** should be addressed to Camille Lange, Frank Maldarelli or Irini Sereti. clange@hivresearch.org; fmalli@mail.nih.gov; isereti@niaid.nih.gov.

Author contributions

A.L., C.M.L., F.M. and I.S. conceived and planned the experiments. A.L., M.M., S.K., D.A.H. and I.S. provided clinical care. A.L., C.M.L., S.K., R.D., R.J.G., Q.Y., D.H., N.L., P.Y., K.B. and C.M.F. carried out the experiments. C.M.L., A.L., B.R., C.R., B.S., C.S., R.J.G., K.H. and N.L. contributed to sample preparation. A.L., C.M.L., M.M., F.M., I.S., R.J.G., B.K., C.M.F. and P.M. contributed to the interpretation of the results. C.M.L. took the lead in writing the initial draft of the manuscript. All authors provided critical feedback and helped shape the research, analysis and manuscript.

Online content

Any methods, additional references, Nature Portfolio reporting summaries, source data, extended data, supplementary information, acknowledgements, peer review information; details of author contributions and competing interests; and statements of data and code availability are available at https://doi.org/10.1038/s41591-023-02387-4.

Competing interests

The authors declare no competing interests.

Additional information

Supplementary information The online version contains supplementary material available at https://doi.org/10.1038/s41591-023-02387-4.

Peer review information *Nature Medicine* thanks Janice Clements and the other, anonymous, reviewer(s) for their contribution to the peer review of this work. Primary Handling Editor: Alison Farrell, in collaboration with the *Nature Medicine* team.

[7]Center for Infectious Disease Imaging, National Institutes of Health Clinical Center, National Institutes of Health, Bethesda, MD, USA.

[8]Section of Infections of the Nervous System, National Institute of Neurological Disorders and Stroke, National Institutes of Health, Bethesda, MD, USA.

[9]Laboratory of Human Retrovirology and Immunoinformatics, Frederick National Laboratory for Cancer Research, Frederick, MD, USA.

[10]Eshelman School of Pharmacy, University of North Carolina at Chapel Hill, Chapel Hill, NC, USA.

[11]Present address: Military HIV Research Program, Walter Reed Army Institute of Research, Henry M. Jackson Foundation for the Advancement of Military Medicine, Silver Spring, MD, USA.

[12]These authors contributed equally: Andrea Lisco, Camille Lange, Frank Maldarelli, Irini Sereti.

Abstract

Reservoirs of HIV maintained in anatomic compartments during antiretroviral therapy prevent HIV eradication. However, mechanisms driving their persistence and interventions to control them remain elusive. Here we report the presence of an inducible HIV reservoir within antigen-specific $CD4^+$T cells in the central nervous system of a 59-year-old male with progressive multifocal leukoencephalopathy immune reconstitution inflammatory syndrome (PML-IRIS). HIV production during PML-IRIS was suppressed by modulating inflammation with corticosteroids; selection of HIV drug resistance caused subsequent breakthrough viremia. Therefore, inflammation can influence the composition, distribution and induction of HIV reservoirs, warranting it as a key consideration for developing effective HIV remission strategies.

HIV reservoir persistence on antiretroviral therapy (ART) is the principal obstacle to HIV eradication. HIV-infected cells are widely anatomically distributed; however, mechanisms driving their distribution and dynamics in vivo remain poorly understood[1,2]. HIV-infected cells in the central nervous system (CNS)[1,2] may represent a critical reservoir during ART, given that persistent and episodic HIV release on effective ART has been observed[3,4]. Understanding the dynamics of immunologic and virologic mechanisms driving HIV persistence in the CNS and other tissue reservoirs is a key consideration in developing scalable strategies for HIV eradication[5]. In this case study, we demonstrate that immune recovery, stimulation and trafficking of antigen-specific $CD4^+$T cells drove HIV persistence, with gradual replacement of HIV reservoirs with ART-resistant proviruses. Furthermore, HIV production from viral reservoirs was directly modulated by corticosteroids, implicating inflammation in HIV reservoir dynamics.

A 59-year-old man was diagnosed with HIV-associated acquired immunodeficiency syndrome after presenting with *Pneumocystis jirovecii* pneumonia (PJP), cytomegalovirus (CMV) colitis, $CD4^+$T cell count of 16 cells per microliter and plasma HIV viral load (HIV VL) of 2,109,306 copies per milliliter. He was referred to the National Institutes of Health (NIH) Clinical Center, having met enrollment criteria for the ART-naive arm of the protocol NCT02147405 (≥18-year-old people living with HIV, with CD4 counts ≤100 cells per microliter and ART-naive), a study designed to identify predictors and

optimal management of immune reconstitution inflammatory syndrome (IRIS). Baseline brain magnetic resonance imaging (MRI) noted subtle right thalamic and periventricular hyperintensities without parenchymal or meningeal enhancement. Cerebrospinal fluid (CSF) had 1,200 copies per milliliter of HIV RNA, a normal white cell count and undetectable cryptococcal antigen, CMV, varicella zoster virus, herpes simplex virus-1 and John Cunningham virus (JCV) DNA.

Before ART initiation, HIV drug resistance mutations (DRMs) were not detected in RNA extracted from plasma or lymph nodes via next-generation sequencing (NGS) (Supplementary Fig. 1). PJP and CMV colitis were treated, and ART (elvitegravir/cobicistat/tenofovir-alafenamide/emtricitabine (EVG/COBI/TAF/FTC)) was initiated, resulting in typical multiphasic HIV decay kinetics (Fig. 1a and Supplementary Fig. 2). At 15 weeks after ART initiation, both plasma and CSF HIV VLs were <40 copies per milliliter, and $CD4^+$T cells increased to 307 cells per microliter (Fig. 1a); however, new left-sided ataxia, weakness and dysmetria appeared. MRI and positron emission tomography/computed tomography (PET/CT) findings were consistent with unmasking PML-IRIS: multiple punctate foci of contrast enhancement tracked along the cortical-thalamic-cerebellar pathways involving the right centrum semiovale/subcortical, right thalamus, midbrain and left cerebellar white matter with increased 18F-fluorodeoxyglucose (FDG) uptake (Fig. 1b–d). JCV DNA was detected in CSF and urine by quantitative polymerase chain reaction (qPCR) assay (limit of detection: 1,000 genome equivalents per milliliter), and plasma HIV VLs remained suppressed (<40 copies per milliliter). Prednisone was initiated; maraviroc and mirtazapine were added to modulate CCR5-mediated leukocyte trafficking and JCV replication, respectively[6,7]. By 23 weeks, there were significantly fewer parenchymal contrast-enhancing MRI abnormalities. At 34 weeks, few punctate foci of MRI contrast enhancement reappeared in the same locations (Supplementary Fig. 3a–c); however, by 40 weeks, all neurological symptoms resolved, and slow prednisone taper was completed.

At 54 weeks, new left hand tremor developed with faint MRI contrast enhancement in previously identified foci (Supplementary Fig. 3d), and new CSF lymphocytic pleocytosis (64 cells per microliter, 92% lymphocytes) with elevated HIV VLs (15,493 copies per milliliter of CSF and 185 copies per milliliter of plasma) were documented. JCV DNA was undetectable in CSF; however, given the limitations of the JCV qPCR assay and negative additional infectious workup, relapsed PML-IRIS was diagnosed. Oral prednisone (60 mg d^{-1}) was re-initiated, with clinical and radiological improvement. Within 4 weeks, there were brisk declines in CSF and plasma HIV VLs (68 copies per milliliter and <40 copies per milliliter, respectively); the >200-fold decrease in CSF HIV VL occurred with anti-inflammatory corticosteroid therapy alone, without ART modifications. Complete resolution of neurologic symptoms accompanied disappearances of MRI contrast-enhancing foci (Fig. 1e,f) and normalization of FDG uptake on brain PET/CT by 78 weeks and 96 weeks, respectively (Fig. 1g).

To identify immunological and virological characteristics of PML-IRIS, we retrospectively analyzed CSF and blood samples for JCV-specific T cell responses and HIV population dynamics. Antigen stimulation studies of peripheral blood mononuclear cells (PBMCs) and CSF mononuclear cells revealed robust JCV-specific $CD4^+$T cell responses (Fig.

2a), exceeding responses induced by Epstein–Barr virus (EBV) and CMV antigens (Supplementary Fig. 4). Furthermore, phylogenetic and population subdivision analyses revealed that HIV populations were diverse (Supplementary Table 1), and HIV DNA populations circulating from 24 weeks to 46 weeks were genetically distinct from HIV RNA populations in pre-ART viremia (probability of panmixia $P < 10^{-5}$ and Slatkin–Maddison $P < 0.01$; Supplementary Table 1). Therefore, pre-ART HIV DNA populations derived from PBMCs underwent marked population shifts by the time the first PML-IRIS event occurred.

To determine if JCV-specific $CD4^+$T cells were HIV-infected, we measured total HIV DNA levels in cells proliferating upon JCV peptide pools stimulation ($CFSE^{low}$). HIV DNA levels in $CFSE^{low}$ cells before (46 weeks) and after (96 weeks) relapsed PML-IRIS were similar (820 and 860 HIV DNA copies per 10^6 memory cells, respectively; Supplementary Table 2); however, the relative amount of HIV RNA transcribed from these cell populations at 46 weeks was three times the levels at 96 weeks (cell-associated (CA) HIV RNA:DNA ratios of 80 versus 30, respectively; Supplementary Table 2), demonstrating that JCV antigen-driven induction of HIV proviruses was greater during PML-IRIS. Ex vivo stimulation of memory $CD4^+$T cells with JCV peptide pools in the presence of antiretrovirals resulted in intracellular HIV-1-$p24^+$-*gag* double-positive staining (Supplementary Fig. 5), indicating that p24-Gag protein expression was not the result of spreading infection but, rather, induction of proviral HIV DNA. Therefore, we concluded that peripherally circulating JCV-specific $CD4^+$T cells included inducible HIV reservoirs. When PML-IRIS relapsed, expansion and recruitment of JCV-specific $CD4^+$T cells to the CNS were also associated with antigen-driven activation of HIV-infected memory $CD4^+$T cells, resulting in elevated CSF HIV VLs. Taken together, these data suggest that broad shifts in composition of HIV-infected $CD4^+$T cell populations at PML-IRIS included expansion and brisk recruitment of JCV-specific cells to the CNS. The prominent localized inflammation in relapsed PML-IRIS resulted in elevated production of CSF HIV.

Breakthrough viremia is not characteristic of IRIS; therefore, we performed additional analyses to identify factors contributing to virological rebound. We measured levels of the components of the single-pill combination (Stribild) in CSF and plasma to determine if inadequate CNS drug penetration facilitated HIV replication during PML-IRIS. EVG and FTC plasma concentrations before (46 weeks), during (58 weeks) and after (68 weeks) relapsed PML-IRIS were within therapeutic range at >1 $\log_{10}$ above concentrations inhibiting 90–95% of viral replication ($IC_{90/95}$; Supplementary Fig. 6a–d), typical for virological suppression and corroborating ART adherence. In contrast, CSF ART levels were simultaneously lower than in plasma with suboptimal levels of EVG and TFV (Supplementary Fig. 6e–h). Despite prior reports of lower antiretroviral (ARV) levels in CSF[3,8], to our knowledge, this is the first report of CSF ARV levels $<IC_{90/95}$ accompanying a CNS opportunistic infection and an associated inflammatory event, with rebound viremia. Inadequate CSF ART penetration may have facilitated HIV spread, via JCV-activated $CD4^+$T cells in CSF, which then trafficked into systemic circulation.

In the setting of low CSF ARV levels, we characterized HIV DRMs in HIV populations by single-genome sequencing (SGS) and NGS of protease reverse transcriptase (*pro*-RT) and integrase (IN). Before ART, HIV populations were genetically diverse with no DRMs

in CSF, plasma, lymph node or PBMCs detected by NGS or SGS (Fig. 2b, Supplementary Figs. 1 and 6 and Supplementary Table 1). In contrast, most *pro*-RT and IN sequences derived from rebound CSF HIV VL during relapsed PML-IRIS contained genetically linked DRMs (4/5 M184I-RT and E92Q-IN mutants) (Fig. 2b). Although pre-ART DRMs were undetectable, variants containing M184I(ATC) in RT and E92Q in IN were detected in PBMC-derived HIV RNA at 46 weeks of ART, before PML-IRIS relapse (Fig. 2b, Supplementary Fig. 6 and Supplementary Table 1). The typical mutational pathway to M184I is an ATG-to-ATA transition; however, in this case, it was due to a rare AT***G***-to-AT***C*** transversion, making it a useful marker to track the emergence of this lineage. CSF-derived and PBMC-derived M184I(AT***C***) variants were highly related (bootstrap value >70), indicating that they had a common origin (Fig. 2b). Not all CSF HIV had DRMs; one of five (20%) was a wild-type (WT) variant similar to other variants without DRMs (Supplementary Fig. 6). Taken together, these data suggest that ART-resistant and WT variants circulating in the periphery trafficked to CSF during the relapsed PML-IRIS event and underwent replication under suboptimal CSF ARV levels, resulting in rebound viremia and systemic distribution of DRM-containing variants. Corticosteroid therapy alone suppressed rebound ART-resistant and WT HIV VLs in CSF and plasma, without modification to ART (Fig. 2a), demonstrating the impact of immunomodulation on viremic control[9].

HIV variants replicating in CSF typically acquire HIV envelope (*env*) features distinct from peripheral blood variants[3,4]. We analyzed *env*-SGS from pre-ART plasma HIV VL and rebound CSF HIV VL (54 weeks) to investigate the source of the CSF HIV. All CSF (30/30) and plasma HIV (16/16) variants were predicted to use CCR5 co-receptors (CCR5 false-positive rate < 10%), yet CSF and plasma HIV populations were distinct. Similar to *pro*-RT populations, CSF and plasma *env* populations were phylogenetically distinct (bootstrap > 95; panmixia probability $P < 10^{-9}$) (Supplementary Fig. 6c), and there were two separate migration events between plasma and CSF HIV populations (Slatkin–Maddison analysis, probability of fewer than two events < 10^{-4}). Additionally, amino acid changes at 13 loci occurred in all CSF variants with significant differences in allele frequencies compared to plasma HIV ($P \leq 10^{-4}$ for all loci, Fisher's exact test) (Supplementary Table 3); there were two changes in the V3 loop and two new acquisitions in the glycan shield (V1 and C4). Overall, these data support the CNS as the site of replication for WT and drug-resistant HIV.

PML-IRIS symptoms progressively improved with a prolonged prednisone taper, which was discontinued at 70 weeks. HIV VLs were intermittently detectable at low levels; however, by 96 weeks, plasma HIV VL increased to 509 copies per milliliter (Supplementary Table 1), and, by 104 weeks, 85–95% of rebound viremia was predominantly drug resistant based on NGS results (Supplementary Fig. 1d). Single-genome analyses demonstrated that HIV drug-resistant variants at 104 weeks were highly related to those detected in rebound CSF HIV VL at 54 weeks during relapsed PML-IRIS and in 23% (3/13) of PBMC HIV RNA populations at 46 weeks (Supplementary Fig. 6). These findings are consistent with trafficking of drug-resistant HIV from CSF to peripheral blood[10], which culminated in a loss of virological control by 104 weeks.

Low-level HIV VLs persisted until 104 weeks, when ART was changed to darunavir/COBI/TAF/FTC, with prompt suppression to <40 copies per milliliter, demonstrating that rebound HIV VL was the product of active HIV replication. The individual remained clinically stable for the next 5 years without further ART failure, and $CD4^+$T cell counts increased to 530 cells per microliter. He underwent research lymph node (117 weeks) and recto-sigmoidal (133 weeks) biopsies that were both histopathologically unremarkable. HIV proviruses were present but infrequent in these tissues: M184I(ATC) and M184V(GTG) were each 0.01% of lymph node HIV DNA sequences (Supplementary Fig. 7). No DRMs were found in recto-sigmoidal tissues (Supplementary Table 1).

Undetectable HIV DRMs before 46 weeks of ART does not negate their existence or selection from pre-ART and post-ART cells and tissues, nor does it infer directionality of trafficking of HIV reservoirs among anatomic compartments before release and outgrowth in the CNS. We propose that the emergence of HIV DRMs resulting in ART failure occurred in the following sequence (Fig. 2c). (1) DRMs emerged before ART initiation as minority variants, as predicted in large replicating WT HIV populations[11], including HIV-infected, JCV-specific memory cells. (2) JCV antigen-driven activation and proliferation of JCV-specific T cells during the first IRIS event facilitated trafficking and expansion of an inducible HIV reservoir in the CNS[12,13]. (3) Antigen-mediated activation of JCV-specific T cells during relapsed PML-IRIS facilitated reactivation of HIV reservoirs in CNS. (4) Corticosteroids reduced inflammation, which controlled reactivation of HIV from their reservoirs during PML-IRIS. (5) Localized replication of restricted, neuro-adapted, CCR5-utilizing HIV population ensued in the CNS where there was suboptimal ART penetration, facilitating the emergence of drug-resistant HIV that disseminated to the periphery. (6) Although corticosteroids initially controlled HIV replication, eventually, minority drug-resistant variants generated substantial rebound viremia after a relatively long time[5].

Initiating ART in advanced HIV/AIDS is common, especially in resource-limited settings, generating large populations at higher risk for IRIS[14]; understanding mechanisms driving IRIS will improve care of these individuals. Expansion and contraction of HIV-infected populations in response to specific antigenic stimuli have been previously reported in peripheral blood[12,15], but their role in IRIS or in anatomic compartments is unknown. In this study, we revealed brisk trafficking of JCV-specific HIV-infected cells across anatomic compartments during PML-IRIS, demonstrating that HIV reservoir reactivation could be manipulated by anti-inflammatory drugs, even in a specific compartment such as the CSF.

The HIV reservoir is a product of dynamic immunologic and virologic forces that determine the composition and distribution of HIV populations. Here we demonstrated that clinical events resulting from specific and measurable immunological forces drive the mutational composition and anatomic distribution of the HIV reservoir. This case study highlights the importance of current efforts to develop immunomodulatory strategies to modulate HIV reservoirs in compartments such as the CNS, including induction of HIV latency reversal in antigen-specific T cells (checkpoint blockade reservoir purging) or prevention of cytokine-driven homeostatic expansion without disrupting effector T cell functions (that is, Janus kinase inhibitors)[16–18]. Ongoing studies will define the potential effects of these immunomodulating strategies on HIV reservoir dynamics during ART[19]. These scalable and

multimodal approaches to modulate immune activation and impact antigen-specific HIV reservoirs will be useful for designing effective HIV remission strategies.

Methods

Study participant and materials

The study participant was referred to the NIH Clinical Center and enrolled in an institutional review board (IRB)-approved prospective observational protocol (NCT02147405) started on 30 May 2014. The participants of the protocol are people with HIV-1 infection who are naive to ART, have a $CD4^+$T cell count <100 cells per microliter and agree to be followed for at least 96 weeks after ART initiation, with the opportunity to extend such follow-up as clinically indicated. The study participant, a 59-year-old male, provided written informed consent in accordance with the Declaration of Helsinki. PBMCs were purified by density gradient centrifugation from heparinized blood. Plasma collected from EDTA-treated tubes after centrifugation for 15 min at 2,000*g* was aliquoted and stored at −80 °C. CSF was collected in clinically indicated lumbar puncture procedures. CSF mononuclear cells were obtained by centrifugation at 400*g* and freshly used in assays evaluating JCV antiviral activity. CSF supernatant was aliquoted and stored at −80 °C for downstream virological and immunological analysis.

JCV-, EBV- and CMV-specific T cell responses in peripheral blood and CSF

JCV-, EBV- and CMV-reactive T cells were generated using commercially available overlapping peptide libraries against immunodominant viral antigens obtained from commercial vendors (JPT and Miltenyi Biotec). Fresh peripheral blood and CSF mononuclear cells were pulsed with peptide libraries (final concentration of 1 μg ml^{-1}). Irrelevant peptide NY-ESO1 (New York esophageal squamous cell carcinoma 1) was used as a negative control, and a peptide mix of CMV (pp65, immediate early 1 (IE1)) and EBV (Epstein–Barr nuclear antigen (EBNA), BamHI Z fragment leftward open reading frame 1 (BZLF1)) was used to compare specific T cell responses against other viruses in PBMCs. Cells were suspended in AIM-V media (Thermo Fisher Scientific) supplemented with inactivated 5% human serum, IL-7 and IL-15 (10 ng ml^{-1}, PeproTech) and plated on 96-well U-bottom plates. Cultures were maintained, fed and split as needed every 3 d for approximately 14 d, with IL-2 (30 IU ml^{-1}, PeproTech) added 72 h after the initial stimulation. Cultures were then re-stimulated with the same peptide libraries for 4–6 h in the presence of brefeldin A and monensin A (BD Biosciences) to prevent cytokine degranulation per the manufacturer's instructions. Intracellular cytokine production was measured by flow cytometry. Cells were prepared using BD Cytofix/Cytoperm Kit following the manufacturer's instructions. The following surface markers and cytokines were analyzed with CD3, CD4, CD8, TNFα and IFNγ antibodies (BioLegend, 300407; BD Biosciences, 562843; BD Pharmingen, 555369; BD Biosciences, 557647; and BD Biosciences, 554669, respectively) with Vivid fixable violet amine reactive dye for viability (Invitrogen/Molecular Probes).

JCV antigen-specific CD4$^+$T cell responses in peripheral blood

Thawed PBMCs from weeks 46 and 96 after ART were first resuspended in RPMI 1640 supplemented with 10% human AB serum, 50 μg ml^{-1} gentamicin and 1.7 mM L-glutamine and then rested for 1 h at 37 °C in the presence of 125 U ml^{-1} benzonase (Sigma-Aldrich). To identify CD4$^+$T cells that were JCV antigen specific, PBMCs were first labeled with 10 μM carboxyfluorescein succinimidyl ester (CellTrace, Thermo Fisher Scientific, C34554) to monitor cellular proliferation and were then stimulated by JCV peptide mix (VP1 and large T antigen, 0.4 μg ml^{-1}, Peptides and Elephants). Cells were plated at 3 × 10^6 cells per well in a 96-well deep-well plate and cultured for 6 d with JC Peptide Pools and 1 μg ml^{-1} of co-stimulatory antibodies αCD28 and αCD49d. Three different independent experiments were performed in the presence of different ART regimens (darunavir/nevirapine (5 μM of each drug, Sigma-Aldrich); raltegravir 200 nM; and raltegravir 200 nM + 3 IU ml^{-1} of IL-2). Non-naive CD4$^+$T cells were identified by extracellular staining and then sorted into CFSE^{high}/CFSE^{low} subsets. CFSE^{low} subsets identified JCV antigen-specific, non-naive CD4$^+$T cells that underwent antigen-driven proliferation in response to the JC peptide mix stimulation. Anti-CD3-PE, anti-CD4-BV605, anti-CD8-APC, anti-CD27-BV711 (BioLegend, 302833) and anti-CD45RO-PE-Cy7 (BD Biosciences, 337168) were used for T cell staining. Dead cells were identified and excluded using LIVE/DEAD Fixable Near IR Dead Cell Stain Kit (Thermo Fisher Scientific, L34976). See Supplementary Fig. 4b for gating strategy. CA HIV-1 measurements were performed as described below.

HIV RNA and DNA levels in CSF, PBMC and plasma

Plasma and PBMC were obtained before and after ART initiation. PBMCs, CSF and tissue from the lymph node, sigmoid and rectum were obtained during the first 2 years of ART. Viral RNA was extracted from plasma by isopropanol/ethanol precipitation, and CA DNA and RNA were isolated with TRIzol from cells and tissue[20]. CA HIV *gag* RNA and DNA levels were measured with single-copy assays using the primers and probe described in Somsouk et al.[21].

HIV-1 p24$^+$ production in JCV antigen-specific CD4$^+$T cells (HIV Flow)

CFSE$^{high/low}$ non-naive CD4$^+$T cells after stimulation with JCV peptides were sorted, centrifuged at 1,500 r.p.m. for 5 min, resuspended at 4 × 10^6 cells per milliliter in culture media (10% human AB serum, 0.02 M lamivudine, 200 nM raltegravir, 300 U ml^{-1} IL-2, 0.5 μl ml^{-1} benzonase) and split into two wells on a 96-well plate. Anti-CD3-BUV395 (BD Biosciences, 563546), anti-CD4-BUV737 (BD Biosciences, 612748), anti-CD8-Pacific Blue (BD Biosciences, 558207), anti-CD27-BV605 (BioLegend, 302830) and anti-CD45RO-PE-Cy7 were used for sorting. An equal volume of media containing either 1:1 pre-washed Dynabeads Human T-Activator CD3/CD28 (Gibco, 11161D) or DMSO control was included. We adapted the HIV-Flow method[22], stimulating cells with the Dynabeads for 42 h and then transferring them to a 5-ml FACS tube, centrifuging at 1,500 r.p.m. for 5 min and aspirating the supernatant. Cell pellets were resuspended in 200 μl of PBS containing 1:1,000 LIVE/DEAD Aqua, CD45RO-ECD (Beckman Coulter, IM2712U), PD1-BV605 (BioLegend, 329923), CD27-BV711 and CXCR5-BV421 (BioLegend, 356919) and incubated for 30 min at room temperature. Cells were then fixed and permeabilized

(Foxp3 transcription buffer stain, eBiosciences) for 30 min at room temperature. After permeabilization, cells were stained with CD4-PE-Cy7 (Life Technology, 25-0042-82), CD3-BUV395 (BD Biosciences, 563546), p24 KC67-PE (Beckman Coulter, CO6604667) and p24 28B7-APC (MédiMabs, MM-0289-APC) for 45 min at room temperature. Cells were acquired using a Fortessa II flow cytometer (BD Biosciences) and analyzed using FlowJo version 10 software. See Supplementary Fig. 4c for gating strategy.

MRI

MRI was performed on 3-T scanners per clinical routine at our site and included administration of gadolinium-based contrast material (0.1 mmol kg^{-1} gadoteridol, ProHance or gadobuterol, Gadavist). T1-weighted, T2-weighted and post-contrast three-dimensional T1-weighted and fluid-attenuated inversion recovery (FLAIR) images were reviewed.

PET/CT

PET/CT scans of the brain were obtained 60 min after the administration of approximately 10 mCi of FDG intravenously. Reconstructed, attenuation-corrected images were reviewed.

Plasma and CSF ARV concentrations

ARVs were extracted from plasma and CSF by protein precipitation with methanol containing stable, isotopically labeled $^{13}C_5$-TFV, $^{15}N,d_2$-FTC, d_6-MVC and d_6-EVG as internal standards. Concentrations were determined by liquid chromatography–tandem mass spectrometry assays with dynamic ranges of 1–4,000 ng ml^{-1} TFV and FTC, 1–10,000 ng ml^{-1} MVC and 2–10,000 ng ml^{-1} EVG. Biological concentrations were compared longitudinally as well as compared to 90% and 95% ICs reported in treatment-experienced adults (Gilead Sciences (2016), GENVOYA: Highlights of Prescibing Information, FDA reference: 4023346; ViiV Healthcare (2016), SELZENTRY: Highlights of Prescibing Information, FDA reference 4009160).

SGS

Single-genome sequences encoding HIV *pro*-RT (982 nucleotides) and HIV IN (680 nucleotides) and near-full-length envelope (*env*) were obtained from viral populations in plasma, cells and/or tissue[23,24] (see Supplementary Table 1b for sequencing primers). Sequence analyses were performed with Version X of the Molecular Evolutionary Genetic Analysis Software (MEGA X; https://www.megasoftware.net). APOBEC3G/F hypermutated sequences were identified with Hypermut 4.0 (https://www.hiv.lanl.gov/content/sequence/HYPERMUT/hypermut.html) and excluded from sequence analyses.

HIV phylogenetic analyses

Clinical assessment of HIV drug resistance (DR) was determined at the NIH Clinical Center. NGS from plasma-derived samples was performed with the MiSeq system (Illumina), and HIV DRMs were detected with VISL (variants in susceptibility loci). NucAmino was used to determine ambiguity at codon 184 in reverse transcriptase (5–15% threshold) (https://github.com/hivdb/NucAmino). DRMs were identified with Stanford University's HIV Drug Resistance Database (https://hivdb.stanford.edu/hivdb/by-mutations/). MEGA X

was used to determine average pairwise distances (APDs) and reconstruct phylogenies. The relatedness of viral variants was depicted with Neighbor-Joining (NJ) trees. To investigate whether HIV populations underwent shifts, geographic subdivision and Slatkin–Maddison tests were performed. We compared HIV lineages to pre-therapy plasma RNA populations (≥10 lineages per population were compared when duplicate sequences were collapsed to one, representing their lineage). CCR5 co-receptor utilization of *env* sequences was determined with Geno2pheno[coreceptor] (https://coreceptor.geno2pheno.org/) using a false-positive rate of 10%. Parametric and non-parametric compartmentalization analyses were performed with Slatkin–Maddison tests using HyPhy version 2.2.4 (https://www.hyphy.org/) and geographic subdivision analyses[25] (https://bioinfo.mnhn.fr/abi/people/achaz/hudsontest.html).

Statistics

Geographic subdivision analyses were performed as non-parametric comparisons of pairwise distances between 100,000 randomized pairs of intra-patient sequences, generating *P* value for the probability that the randomized populations' structures were the same between sets of sequences, with significance cutoff level of $P < 10^{-9}$. Slatkin–Maddison parametric bootstrapping tests were performed where simulated, and observed frequency distributions of parsimony steps (*s*) of each population member were determined for 1,000 generations in phylogenetic structures of unique sequences. The model was rejected when the observed *s* fell outside of the 95% confidence interval of the simulated distribution with a significance cutoff level of $P < 0.01$. Two-sided Fisher's exact tests were used to compare amino acid frequency of dominant alleles in CSF HIV-1 populations compared to those detected in plasma.

Reporting summary

Further information on research design is available in the Nature Portfolio Reporting Summary linked to this article.

Supplementary Material

Refer to Web version on PubMed Central for supplementary material.

Acknowledgements

The authors thank the staff of the National Institutes of Health (NIH) Clincal Center inpatient and outpatient services, the National Institute of Allergy and Infectious Diseases research staff and the study participant for their important contributions, without whom this research would not have been possible. We also thank E. Bruzzesi for contributions in the laboratory. This research was supported, in part, by the Intramural Research Program of the NIH and, in part, with federal funds from the National Cancer Institute under contract number 75N91019D00024/HHSN261201500003I as well as the Office of AIDS Research under the strategic funds supplement: 'Impact of lymphopenia and co-infections on residual inflammation and reservoirs'. The content of this publication does not necessarily reflect the views or policies of the Department of Health and Human Services, nor does mention of trade names, commercial products or organizations imply endorsement by the US government.

Data availability

pro-RT, IN and *env* sequences are publicly available (GenBank accession numbers OQ924993-OQ925343, OM937385-OM937739 and OQ925344-OQ925389, respectively). All other data are included in the paper and supplementary documents.

References

1. Bozzi G et al. No evidence of ongoing HIV replication or compartmentalization in tissues during combination antiretroviral therapy: implications for HIV eradication. Sci. Adv 5, eaav2045 (2019). [PubMed: 31579817]
2. Chaillon A et al. HIV persists throughout deep tissues with repopulation from multiple anatomical sources. J. Clin. Invest 130, 1699–1712 (2020). [PubMed: 31910162]
3. Joseph SB et al. Human immunodeficiency virus type 1 RNA detected in the central nervous system (CNS) after years of suppressive antiretroviral therapy can originate from a replicating CNS reservoir or clonally expanded cells. Clin. Infect. Dis 69, 1345–1352 (2019). [PubMed: 30561541]
4. Woodburn BM et al. Characterization of macrophage-tropic HIV-1 infection of central nervous system cells and the influence of inflammation. J. Virol 96, e0095722 (2022). [PubMed: 35975998]
5. Deeks SG et al. Research priorities for an HIV cure: International AIDS Society Global Scientific Strategy 2021. Nat. Med 27, 2085–2098 (2021). [PubMed: 34848888]
6. Giacomini PS et al. Maraviroc and JC virus-associated immune reconstitution inflammatory syndrome. N. Engl. J. Med 370, 486–488 (2014). [PubMed: 24476450]
7. Mullins C, Miranda J, Sandoval H, Ramos-Duran L & Tonarelli SB The benefit of mirtazapine in the treatment of progressive multifocal leukoencephalopathy in a young HIV-positive patient: a case report. Innov. Clin. Neurosci 15, 33–35 (2018).
8. Gele T et al. Cerebrospinal fluid exposure to bictegravir/emtricitabine/tenofovir in HIV-1-infected patients with CNS impairment. J. Antimicrob. Chemother 76, 3280–3285 (2021). [PubMed: 34508640]
9. Gunst JD, Hojen JF & Sogaard OS Broadly neutralizing antibodies combined with latency-reversing agents or immune modulators as strategy for HIV-1 remission. Curr. Opin. HIV AIDS 15, 309–315 (2020). [PubMed: 32675575]
10. Wiegand A et al. Single-cell analysis of HIV-1 transcriptional activity reveals expression of proviruses in expanded clones during ART. Proc. Natl Acad. Sci. USA 114, E3659–E3668 (2017). [PubMed: 28416661]
11. Coffin JM HIV population dynamics in vivo: implications for genetic variation, pathogenesis, and therapy. Science 267, 483–489 (1995). [PubMed: 7824947]
12. Simonetti FR et al. Antigen-driven clonal selection shapes the persistence of HIV-1-infected CD4+ T cells in vivo. J. Clin. Invest 131, e145254 (2021). [PubMed: 33301425]
13. Kincer L et al. HIV-1 is transported into the central nervous system by trafficking infected cells. Pathog. Immun 7, 131–142 (2023). [PubMed: 36865569]
14. Sereti I et al. Prospective international study of incidence and predictors of immune reconstitution inflammatory syndrome and death in people living with human immunodeficiency virus and severe lymphopenia. Clin. Infect. Dis 71, 652–660 (2020). [PubMed: 31504347]
15. Mendoza P et al. Antigen-responsive CD4+ T cell clones contribute to the HIV-1 latent reservoir. J. Exp. Med 217, e20200051 (2020). [PubMed: 32311008]
16. Gavegnano C et al. Novel mechanisms to inhibit HIV reservoir seeding using Jak inhibitors. PLoS Pathog 13, e1006740 (2017). [PubMed: 29267399]
17. Uldrick TS et al. Pembrolizumab induces HIV latency reversal in people living with HIV and cancer on antiretroviral therapy. Sci. Transl. Med 14, eabl3836 (2022). [PubMed: 35080914]
18. Chiu CY et al. Combination immune checkpoint blockade enhances IL-2 and CD107a production from HIV-specific T cells ex vivo in people living with HIV on antiretroviral therapy. J. Immunol 208, 54–62 (2022). [PubMed: 34853078]

19. Hsu DC, Mellors JW & Vasan S Can broadly neutralizing HIV-1 antibodies help achieve an ART-free remission? Front. Immunol 12, 710044 (2021). [PubMed: 34322136]

20. Simonetti FR et al. Clonally expanded CD4+ T cells can produce infectious HIV-1 in vivo. Proc. Natl Acad. Sci. USA 113, 1883–1888 (2016). [PubMed: 26858442]

21. Somsouk M et al. The immunologic effects of mesalamine in treated HIV-infected individuals with incomplete $CD4^+$ T cell recovery: a randomized crossover trial. PLoS ONE 9, e116306 (2014). [PubMed: 25545673]

22. Pardons M et al. Single-cell characterization and quantification of translation-competent viral reservoirs in treated and untreated HIV infection. PLoS Pathog 15, e1007619 (2019). [PubMed: 30811499]

23. Palmer S et al. Multiple, linked human immunodeficiency virus type 1 drug resistance mutations in treatment-experienced patients are missed by standard genotype analysis. J. Clin. Microbiol 43, 406–413 (2005). [PubMed: 15635002]

24. Keele BF et al. Identification and characterization of transmitted and early founder virus envelopes in primary HIV-1 infection. Proc. Natl Acad. Sci. USA 105, 7552–7557 (2008). [PubMed: 18490657]

25. Achaz G et al. A robust measure of HIV-1 population turnover within chronically infected individuals. Mol. Biol. Evol 21, 1902–1912 (2004). [PubMed: 15215321]

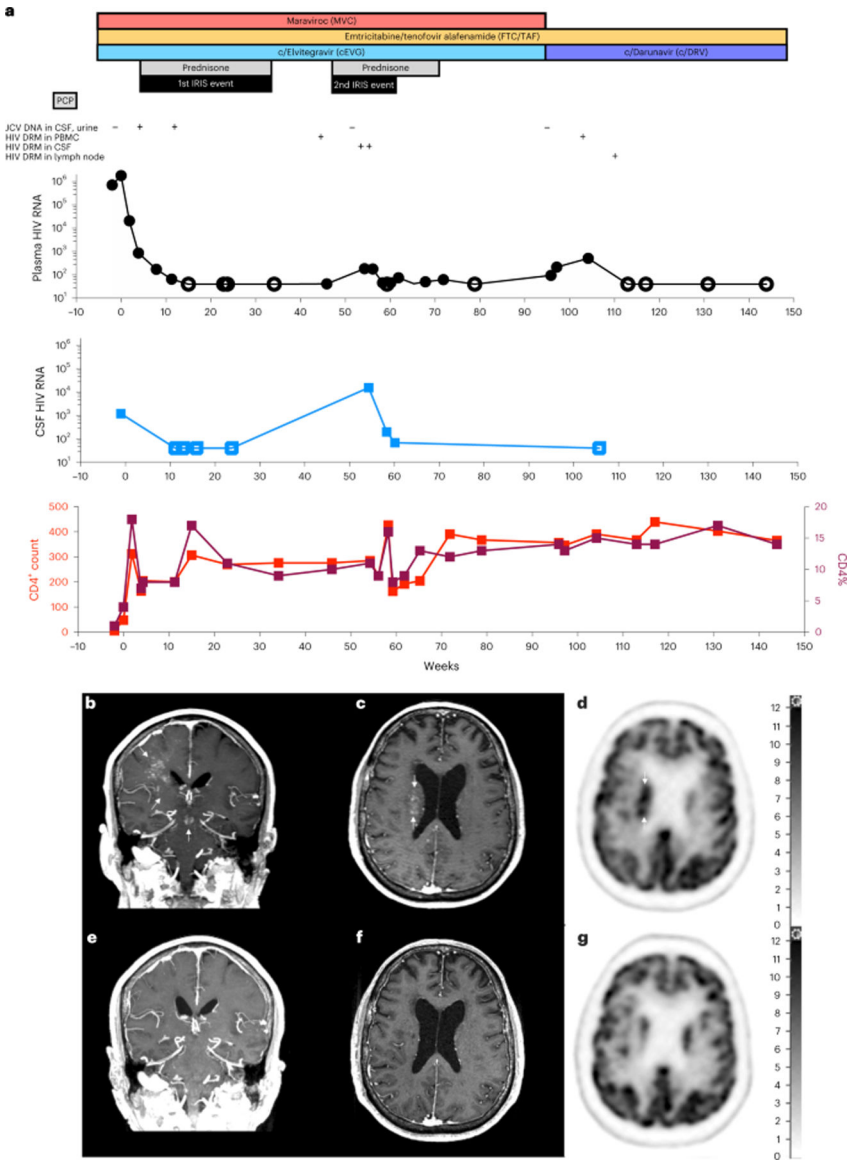

Fig. 1 |. Clinical history.

a, Therapies, JCV DNA, HIV VLs, DRM emergence and CD4^{+}T cell counts. **b**–**g**, Longitudinal brain imaging by post-contrast T1-weighted MRI at 16 weeks (**b**,**c**) with FDG/PET at 12 weeks (**d**), and post-contrast T1-weighted MRI at 78 weeks (**e**,**f**) with FDG/PET scan, at 96 weeks (**g**). Right-sided scale bar: standardized FDG uptake values.

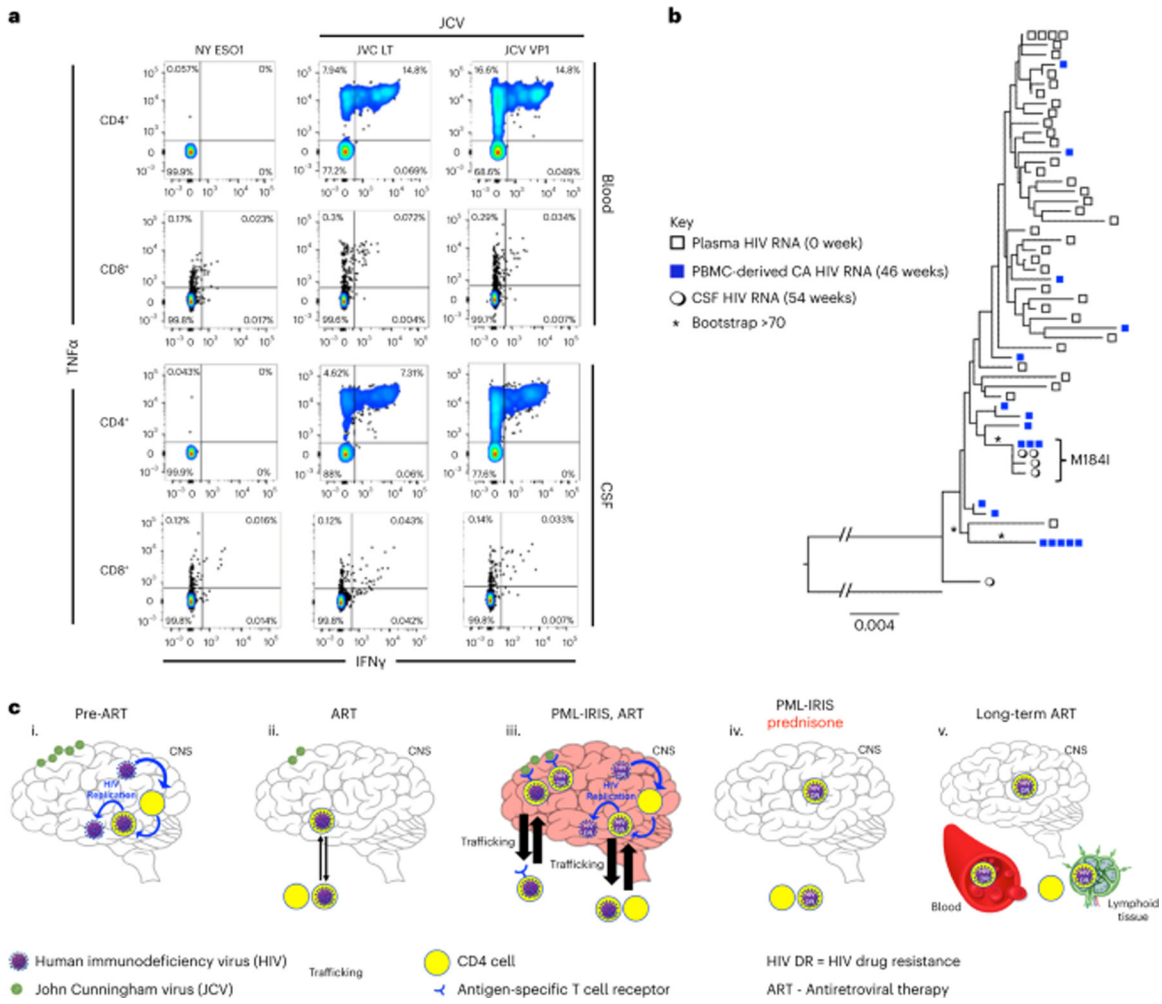

Fig. 2 |. Immunological and virological characteristics of PML-IRIS.

a, JCV-specific T cell responses against a control irrelevant antigen NY-ESO-31, JCV-LT and JCV-VP1 peptide mix. **b**, HIV population structure of pre-ART viremia, cell-associated (CA) HIV RNA at 46 weeks after ART and CSF populations during PML-IRIS at 54 weeks after ART. * indicates bootstrap value >70. Repeating the phylogenetic analysis after removal of the M184I codon did not change the results of the phylogenetic analysis. **c**, The dynamics of HIV reservoir composition in this case of PML-IRIS is the product of shifts in viral replication and immune responses on ART, modulated by pharmacologic intervention. (i) HIV replication ensues in the CNS before ART initiation with underlying JCV co-infection. (ii) HIV replication is inhibited with ART initiation. There is rapid reconstitution of CD4 cells, including JCV-specific CD4 cells infected with replication-competent HIV. (iii) Recruitment of these JCV-specific T cells in the CNS results in IRIS, which drives a shift in HIV reservoir composition. HIV drug resistance (DR) emerges in the CNS where ART is suboptimal. HIV DR gradually spreads across systemic HIV reservoirs. (iv) Introduction of prednisone extinguishes IRIS and HIV replication resulting from activation of JC-specific T cells. HIV-infected cells are cleared from the CNS with further shifts in CD4 cells and HIV reservoir composition. (v) HIV DR trafficked from CNS to blood resulting in HIV DR replication in the periphery with subsequent ART regimen failure and

redistribution of HIV DR in peripheral tissue reservoirs after optimized long-term ART. Green virions indicate JCV. Blue virions indicate HIV. Enclosed yellow circles indicate CD4 cells. Blue arrows indicate HIV replication. Black arrows indicate trafficking across the blood–brain barrier (BBB). Thicker arrows indicate increased trafficking across the BBB. The red-tinted brain indicates inflammation and immune activation during PML-IRIS.